OPAL Technical Note TNxxx
April 19, 2001

Search for the FCNC decay $Z \rightarrow tq$ in the channel $t \rightarrow \ell\nu b$

G. Azuelos[1], E. Elfgren[1] and G. Karapetian[1]
[1]Univ. de Montréal

Abstract

This note describes the analysis for the search of single top production between $\sqrt{s} = 192$ GeV, and $\sqrt{s} = 209$ GeV, in the top decay channel $t \rightarrow \ell\nu b$.

1 Introduction

This note is a follow-up to a Technical Note, TN 655, where the process of $Z \rightarrow tq$ was studied for a center-of-mass energy of 189 GeV, [1]. The physics motivations were explained and a cut-based method was used to analyze the data. The result was an upper limit of the cross section for the single top production of 0.433 pb at 95% C.L.. Single top production was generated with PYTHIA process 1 [2]. The photon background was also investigated and found to be negligible, leading us to ignore it in this Note.

2 Data selection

The present analysis is performed on data collected in 1999-2000 at $\sqrt{s} = 192 - 209$ GeV. The data has been split into four regions, 192-196 GeV, 200-202 GeV, 204-206 GeV and 207-208 GeV each with an integrated luminosity of approximately 0.1 fb^{-1}. The integrated luminosities were calculated by ROCROS, taking into account miniramps. Detector status cuts are shown in table 2 and the resulting luminosities are given in table 1. Note that for low luminosities, $\sqrt{s} = 203$ GeV and $\sqrt{s} = 209$ GeV the data has been merged with $\sqrt{s} = 202$ GeV and $\sqrt{s} = 208$ GeV respectively.

$\sqrt{s}$ [GeV]	192	196	200	202+203	204	205	206	207	208+209
$\int Ldt$ [pb^{-1}]	28.73	71.06	74.25	38.14	6.54	69.56	16.59	106.4	7.69
$\Sigma \int Ldt$	99.79		112.39		92.69			114.09	

Table 1: Integrated luminosities, after detector cuts, for data collected in 1999-2000

.

	1999-2000							
Detector	CJ	CV	EB	EE	HT	HP	SI	SW
Status	3	3	3	3	3	2	3	3

Table 2: Overview of detector status cuts for the data collected in 1999-2000

.

3 Monte Carlo samples

Table 3 lists the Monte Carlo samples used to simulate the FCNC signal and to evaluate the backgrounds. The photon background has already been found to be negligible, [1]. Single top events are characterized by the presence of a W, a b-quark jet and a light quark jet. Therefore, the principal backgrounds will be due mainly to 4-fermion events, in particular WW and ZZ, but also to QCD events: $Z \to q\bar{q}$.

4 Analysis

The present analysis concentrates on the search for single top events with leptonic decay of the W, i.e. $e^+e^- \to t\bar{q} \to \ell\nu bq$, ($\ell = \mu$ or e). This analysis also accounts implicitly for the leptonic channel $e^+e^- \to t\bar{q} \to \tau\nu bq$, where the τ decays to $\mu\nu_\tau$ or $e\nu_\tau$ since the detectable final state is the same. Kinematically, for a centre of mass energy of 189 GeV, at the partonic level and neglecting initial state and final state radiation, the hard process results in the presence of a low energy (14.4 GeV) c-quark, a b-quark with energy in the range 63.3-74.6 GeV and the two leptons from W decay with energies in the range 20-95 GeV but with a combined energy (W energy) of 101-112 GeV.

Because of the presence of two jets, a hadronic preselection is applied. The Tokyo multihadron (TKMH) flag is chosen, since this selection is less restrictive on the visible shower energy than the LMH2 selection. Indeed, events with a muon, a neutrino and the two quarks in the final state would be rejected too often if the required ratio of visible to total centre of mass energy was higher than the 10% set by the TKMH cuts.

The first part of the analysis deals with lepton identification. The ID119 package is used to identify electrons and muons. The highest energy lepton found in the event is taken as the candidate lepton.

The following leptonic cuts are applied:

- The leptons must be isolated: the total energy around it, in a cone of 10 degrees, must be less than 5 GeV (see fig. 1). This cut ensures that the lepton candidate is not inside a jet, from a b-quark, for example.
- The reconstructed lepton momentum must be in the range 10-90 GeV. This range of energy covers the kinematically allowed region and also accounts for the major part

Process	qq	$llqq$	$qqqq$	$ee\tau\tau$	$eeqq$	FCNC	FCNC	FCNC
Generator	KK2f	grc4f	grc4f	grc4f	grc4f	PYTHIA	PYTHIA	PYTHIA
m_{top}	—	—	—	—	—	169 GeV	174 GeV	179 GeV
192 GeV	*5195*	*8750*	*8751*	*9276*	*9277*	—	—	—
# events	100000	44735	43285	9113	100000	—	—	—
196 GeV	*5196*	*9096*	*9097*	*9279*	*9280*	—	*10552*	—
# events		45700	44082	8984	100000	—	19362	—
200 GeV	*5119*	*9313*	*9314*	*9317*	*9318*	—	*10554*	—
# events	200000	46385	44545	8898	197391	—	18943	—
202 GeV	*5199*	*9711*	*9712*	*9808*	*9713*	—	*10554*	—
# events	200000	46595	44722	8763	195239	—	18943	—
204 GeV	*5192*	*10344*	*10345*	*10707*	*10708*	—	—	—
# events	100000	46866	44780	8730	50000	—	—	—
205 GeV	*5183*	*11213*	*11214*	*11217*	*11218*	—	—	—
# events	100000	46952	44834	8697	100000	—	—	—
206 GeV	*5193*	*10070*	*10071*	*10074*	*10075*	*10648*	*10555*	*10654*
# events	79461	47015	44870	8201	191193	20000	20000	20000
207 GeV	*5190*	*10781*	*10782*	*11211*	*11212*	—	—	—
# events	200000	50000	50000	8657	100000	—	—	—
208 GeV	*5191*	*10346*	*10347*	*10712*	*10713*	—	*10656*	—
# events	150000	47132	44831	8629	50000	—	18352	—

Table 3: Run numbers and number of generated events for the Monte Carlo samples used for the analysis for centre–of–mass energies as in column one (in GeV). For each energy, the run number (in italics) and the number of generated events for each process is shown. The last three columns are the FCNC-generated events with a top mass of respectively 169, 174 and 179 GeV.

of phase space for the leptonic τ decay channel. Figures 2-5 show the reconstructed energy of the candidate leptons for the data and the expected backgrounds.

- In order to reject background from the ZZ process, events having a second isolated lepton of same flavour but opposite charge are rejected if the 2-lepton invariant mass is within the mass of the Z, i.e. $80 < m_{ll} < 100$ GeV. Although this cut is of minor importance, it is included here, together with the other leptonic cuts.

The W is reconstructed as the invariant mass of the lepton candidate with the missing 4-vector which is obtained from the measured missing 3-momentum and assuming the missing mass to be zero.

The presence of a neutrino requires that we demand a minimum value of $p_{\rm miss}$. The same cut is applied as for lepton momenta: $10 < p_{\rm miss} < 90$ GeV where method (a) above

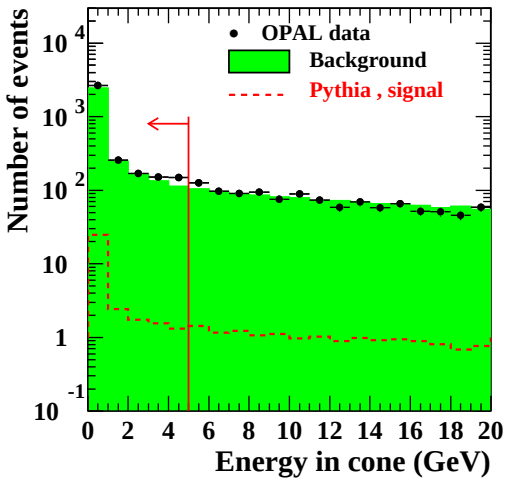

Figure 1: Energy of tracks in a cone of 10° around the candidate lepton for $\sqrt{s} = 204-206$ GeV (the other energy regions being similar). The background is shown as a shaded histogram. The dashed-line histogram is the prediction from PYTHIA, assuming a signal cross-section as given in table 6. Dots are OPAL data. The selected region after the cuts is shown by the arrow.

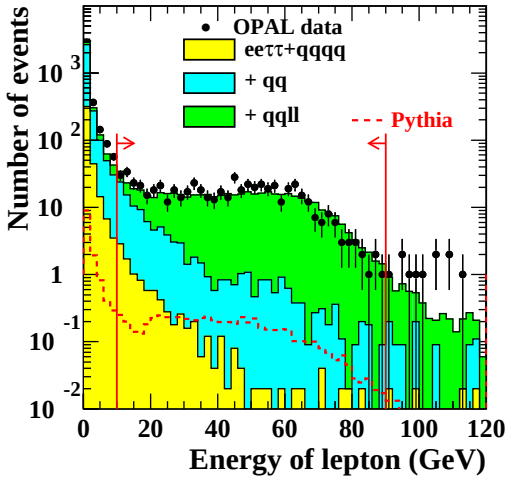

Figure 2: Reconstructed energy of the isolated candidate leptons for $\sqrt{s} = 192-196$ GeV.

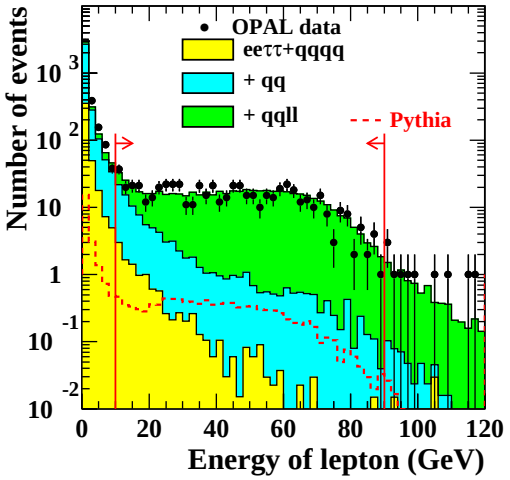

Figure 3: Reconstructed energy of the isolated candidate leptons for $\sqrt{s} = 200-202$ GeV.

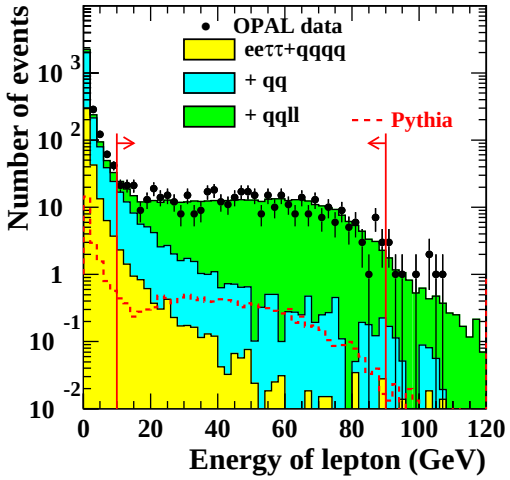

Figure 4: Reconstructed energy of the isolated candidate leptons for $\sqrt{s} = 204-206$ GeV.

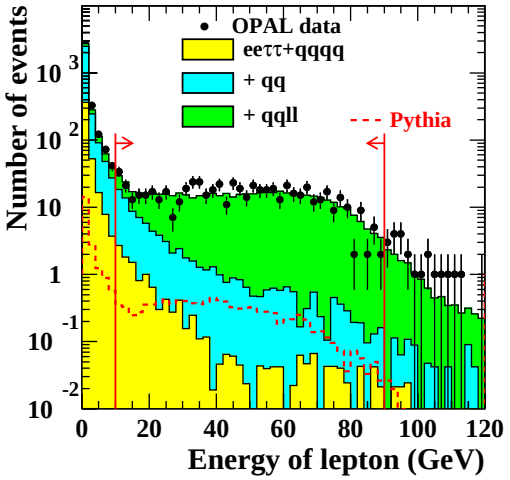

Figure 5: Reconstructed energy of the isolated candidate leptons for $\sqrt{s} = 207-208$ GeV.

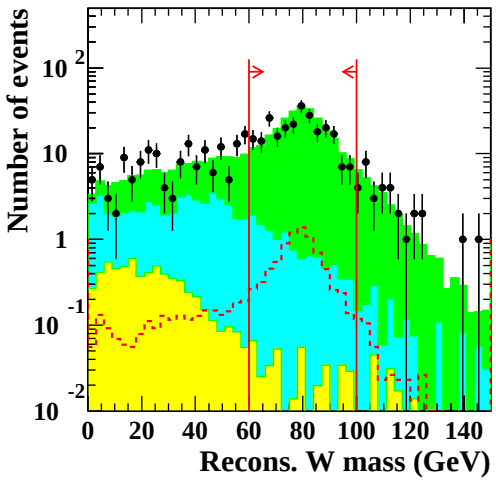

Figure 6: Reconstructed W mass by method (a) for $\sqrt{s} = 204 - 206$ GeV. All previous cuts are applied. Shades of histograms: as in fig. 2.

is used for evaluating $p_{\rm miss}$. The W mass is then reconstructed. Events are accepted if the reconstructed mass, $m_{e\nu}$, is within:

$$60 < m_{e\nu} < 100 \text{ GeV}$$

The signal events are known to have a low-energy light-quark jet and a more energetic b-quark jet. The LB162 b-tagging package [11] is therefore applied. To reconstruct the jets from all tracks and clusters, after having removed the lepton, the MT package is used. Exactly two jets are reconstructed from the hadronic part of the event, using the Durham algorithm. We calculate for each jet (i =1,2) a probability that it is a b-jet using the c-like and u-like outputs of LB:

$$P_b(i) = \frac{1}{c\text{-like}(i) + u\text{-like}(i) + 1} \tag{1}$$

The following jet cuts are applied:

- $y_{12} < y_{12}^{max}$, where y_{12} is the Durham jet resolution parameter at which the number of jets passes from two to one and y_{12}^{max} is given in table 4. This cut is justified in figures 7-8, where it is seen that background from 4 fermion processes (especially $qqll$) can be efficiently rejected.
- The cosine of the visible momentum must be less than 0.9. This is a very efficient cut for $q\bar{q}$ background events, with missing momentum due to initial state radiation to the Z peak, as can be seen in fig. 9.

$\sqrt{s}$ [GeV]	192-196	200-202	204-206	207-208
y_{12}^{max}	0.3	0.35	0.45	0.45

Table 4: Cuts on the y_{12} variable for the different energy regions.

- the reconstructed hadronic mass from the two jets is restricted to avoid the mass region of the W: $m_{\rm hadron} \in \bar{m}_{\rm hadron}$, where $\bar{m}_{\rm hadron}$ is given in table 5 (see figures 10-13). The simple upp limit cut used for $\sqrt{s}192$ is no longer effective for the higher energies. From figures 10-13 one can see that the signal is moving into a high background region. This requires that we cut away the peak of the background, also reducing the signal but proportionally less than the background.

$\sqrt{s}$ [GeV]	192-196	200-202	204-206	207-208
$\bar{m}_{\rm hadron}$	< 75 GeV	20-65, 90-100 GeV	20-65, 90-110 GeV	20-65, 90-120 GeV

Table 5: Cuts on the reconstructed hadronic mass of two jets for the different energy regions.

- The lower energy jet is taken as the candidate c-quark jet and the higher energy jet as the candidate b-jet. The event is rejected if the probability that the candidate b-jet is indeed a b-jet is below 0.4 (see fig 14).

Finally the top quark is reconstructed in two ways:

(i) from the recoil of the candidate c-quark jet.

(ii) from the invariant mass obtained from the 4-vectors of the reconstructed W and of the candidate b-jet.

5 Results

As can be seen in figures 15-18, the width of the reconstructed top mass increases with energy. Therefore we chose an energy dependent window: $166 < m_{top} < 184$ GeV for $\sqrt{s} = 192 - 196$ GeV and $163 < m_{top} < 187$ GeV for the other energy regions.

After the successive application of the above cuts the number of remaining events is shown for the data in column 2, 4, 6, and 8 of table 7. Also shown are the number of events expected from the backgrounds. The cross sections expected for the signal are given in table 6. Figures 15-15 show the final distributions of events, using either method (i) or method (ii) for the top quark reconstruction.

From these results, an upper limit on the cross-section for the single top process can be obtained. We follow the procedure of ref. [12] and find first the upper limit μ on the

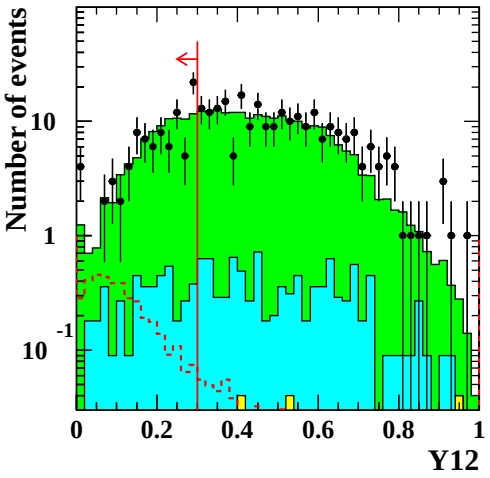

Figure 7: Distribution of parameter y_{12}, the y_{cut} of transition between 1 and 2 jets for $\sqrt{s} = 192-196$ GeV. All previous cuts are applied. Shades of histograms: as in fig. 2.

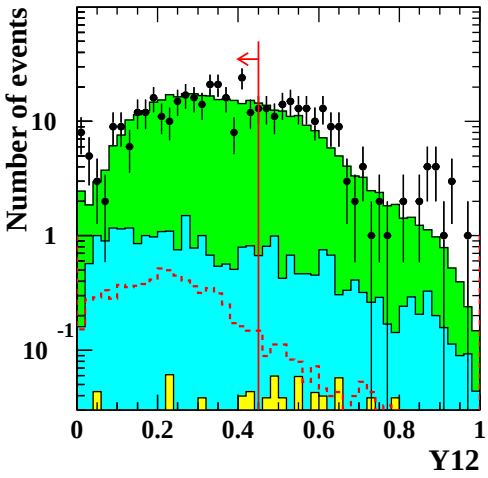

Figure 8: Same as in figure 7 for $\sqrt{s} = 207-208$ GeV.

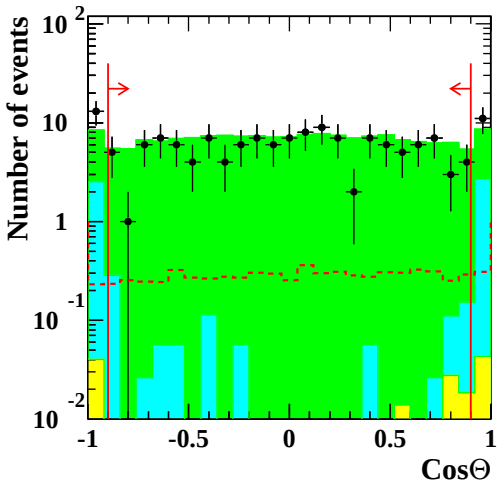

Figure 9: Cosine of the visible momentum for $\sqrt{s} = 204-206$ GeV. All previous cuts are applied. Shades of histograms: as in fig. 2.

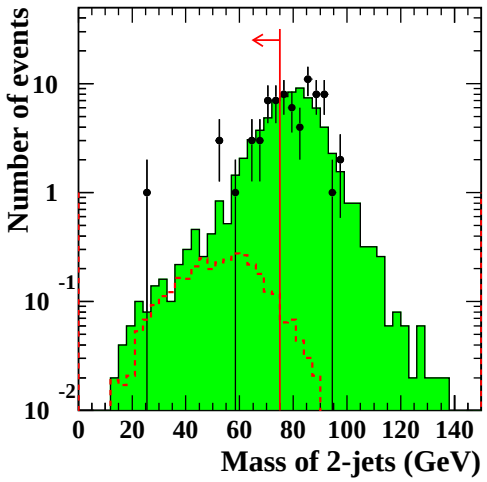

Figure 10: Reconstructed invariant mass of the two-jet system for $\sqrt{s} = 192 - 196$ GeV. All previous cuts are applied. Shades of histograms: as in fig. 2.

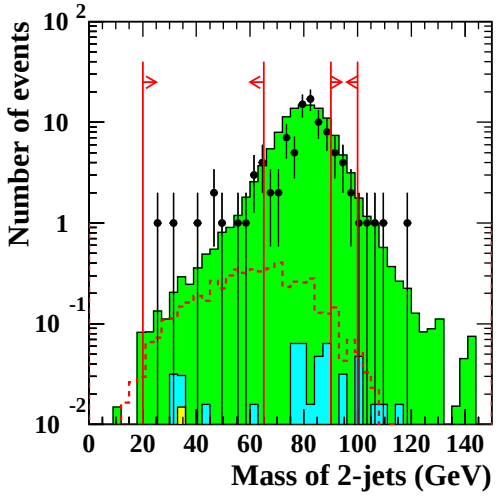

Figure 11: Same as figure 10 for $\sqrt{s} = 200 - 202$ GeV.

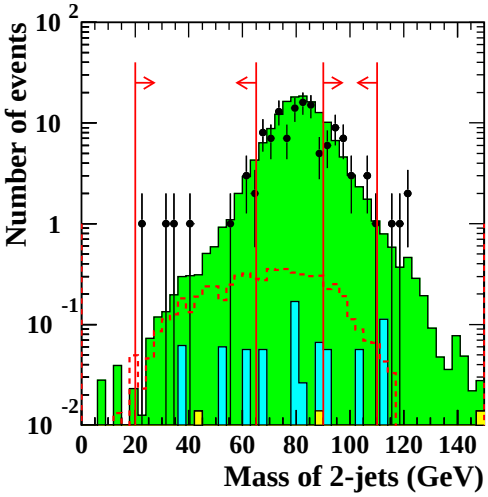

Figure 12: Same as figure 10 for $\sqrt{s} = 204 - 206$ GeV.

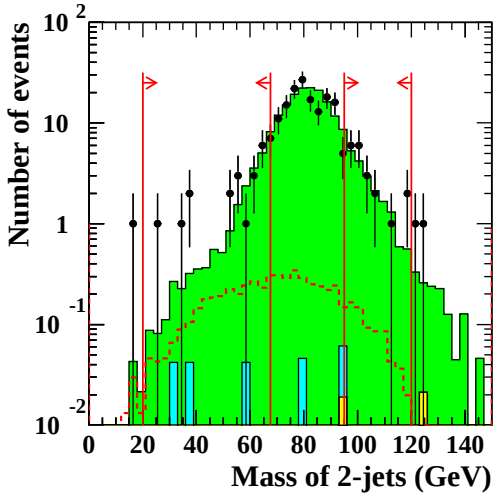

Figure 13: Same as figure 10 for $\sqrt{s} = 207 - 208$ GeV.

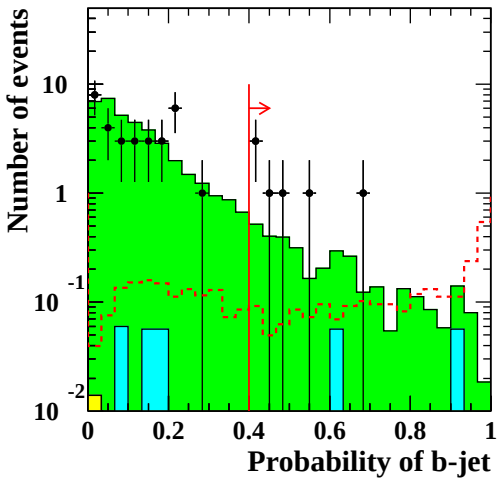

Figure 14: Distribution of b-jet probability for the candidate b-jet for $\sqrt{s} = 204-206$ GeV, as obtained from the LB package. All previous cuts are applied. Shades of histograms: as in fig. 2.

$\sqrt{s}$ [GeV]	192	196	200	202	203	204	205	206	207	208	209
σ_{FCNC} [nb^{-1}]	360	360	600	600	600	600	600	600	600	600	600
$\Sigma\sigma_{FCNC}$	360		600			600			600		

Table 6: Cross sections for the estimated FCNC-process as calculated in [7]

expected value μ_S of signal events, with confidence level α, given an expected background of b events and a number n_0 of events observed. The results are given in table 8.

The stability of this result with respect to the analysis is verified by:

- varying the choice of selection cuts
- use of method (ii) for the reconstruction of the top mass, i.e. the reconstruction of the invariant mass of the $l\nu b$ system. The mass window chosen in this case was $145 < m_t < 187$ GeV.

The results are summarized in table 9.

The following sources of systematic error, have been examined:

- **Monte Carlo simulation**. A comparison between the results obtained with the EXOTIC Monte Carlo sample and with the PYTHIA sample allows an estimate

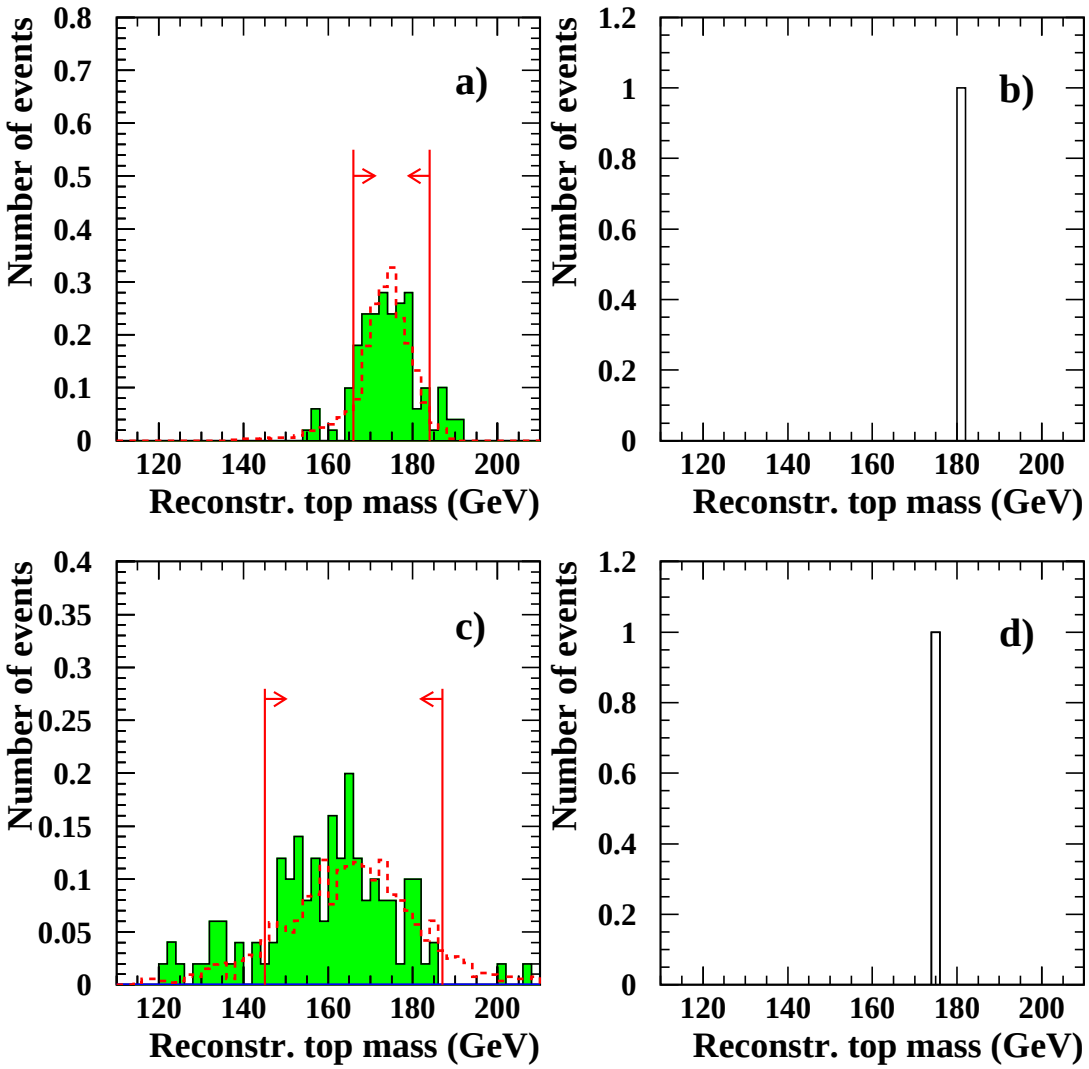

Figure 15: Reconstructed mass of the top candidate events, after application of all cuts for $\sqrt{s} = 192 - 196$ GeV. Histogram shades as in fig. 2. (a) Monte Carlo, method (i); (b) data, method (i); (c) Monte Carlo, method (ii); (d) data, method (ii).

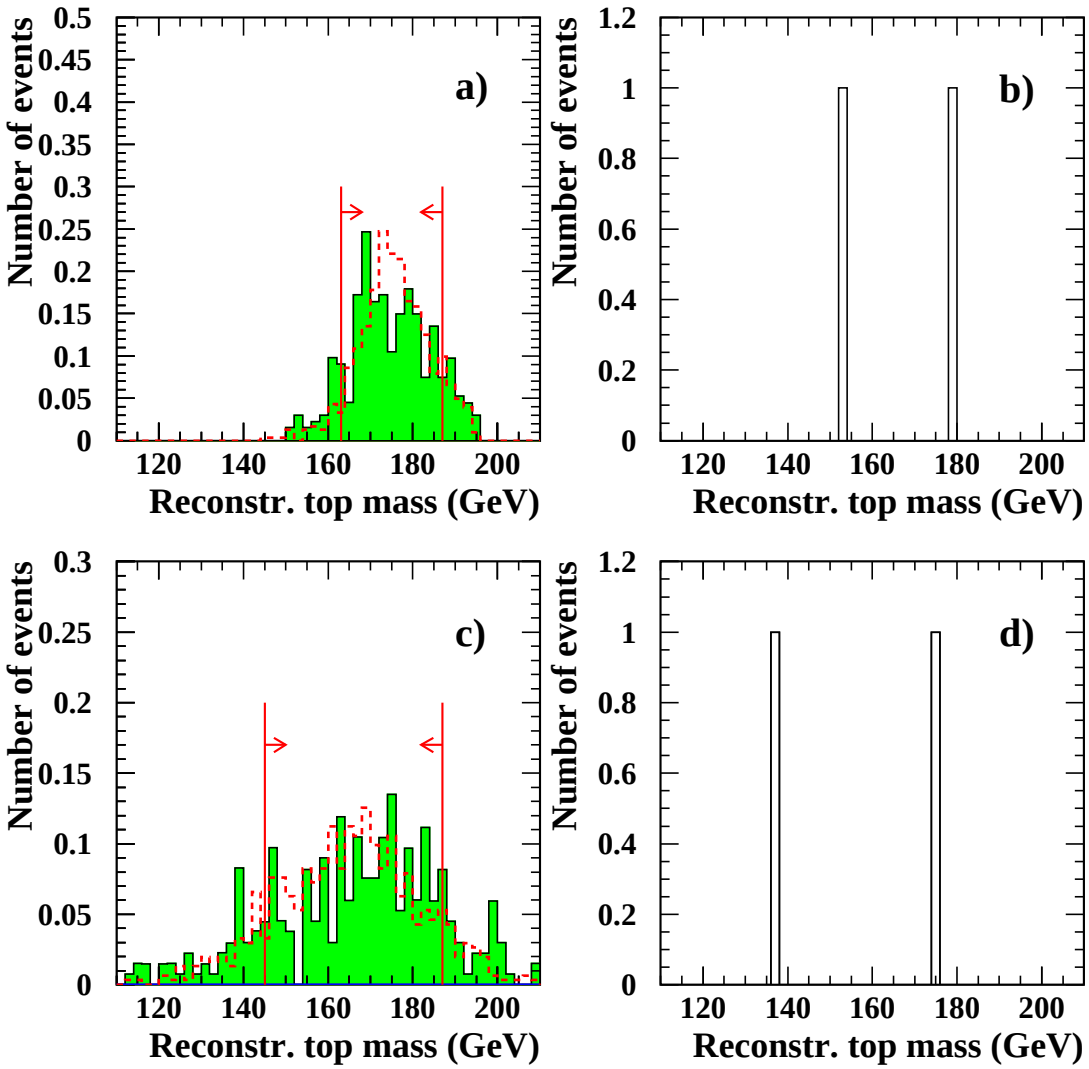

Figure 16: Reconstructed mass of the top candidate events, after application of all cuts for $\sqrt{s} = 200 - 203$ GeV. Histogram shades as in fig. 2. (a) Monte Carlo, method (i); (b) data, method (i); (c) Monte Carlo, method (ii); (d) data, method (ii).

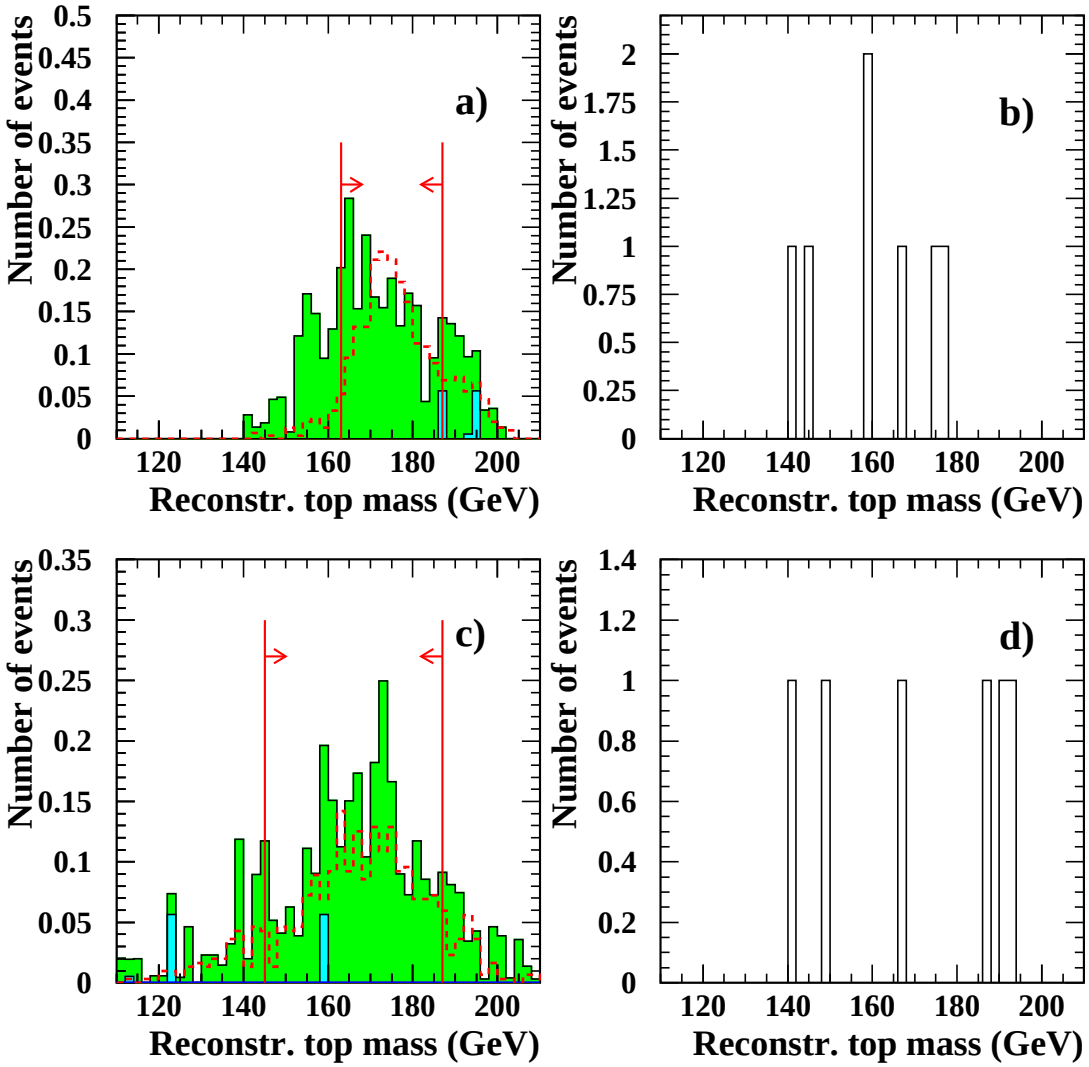

Figure 17: Reconstructed mass of the top candidate events, after application of all cuts for $\sqrt{s} = 204 - 206$ GeV. Histogram shades as in fig. 2. (a) Monte Carlo, method (i); (b) data, method (i); (c) Monte Carlo, method (ii); (d) data, method (ii).

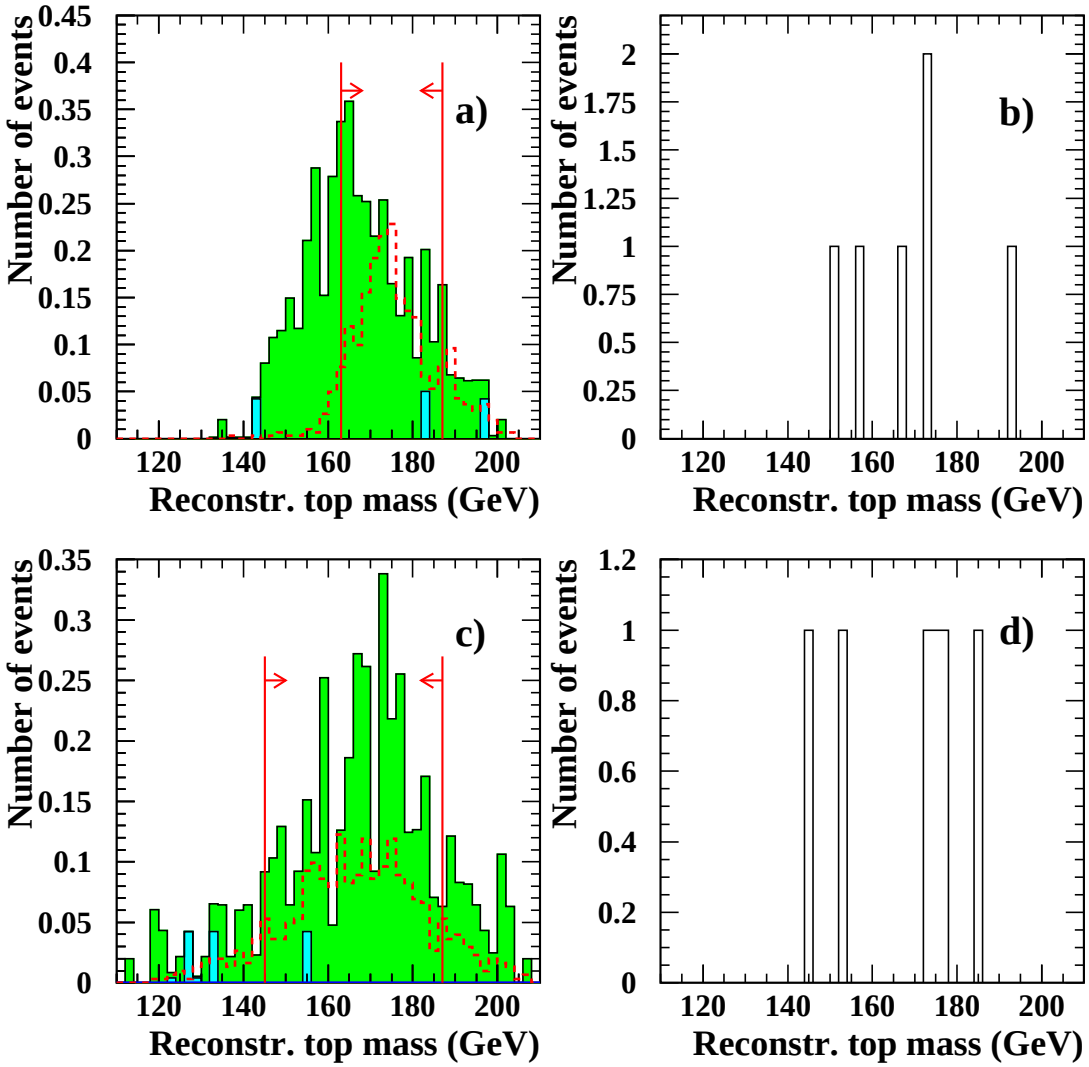

Figure 18: Reconstructed mass of the top candidate events, after application of all cuts for $\sqrt{s} = 207 - 209$ GeV. Histogram shades as in fig. 2. (a) Monte Carlo, method (i); (b) data, method (i); (c) Monte Carlo, method (ii); (d) data, method (ii).

Cut	$\sqrt{s}$=192 –196	Bg	$\sqrt{s}$=200 –202	Bg	$\sqrt{s}$=204 –206	Bg	$\sqrt{s}$=207 –208	Bg
TKMH + 1 ℓ	714	640.4	1456	1500	1374	1204	1631	1401
ℓ isolation	580	491.4	1116	1095	1033	884.8	1216	1038
ℓ energy	112	114.6	197	244.7	207	208.1	280	247.9
2-ℓ mass	112	114.2	196	244.3	205	207.9	280	247.2
missing p	109	111.5	189	238.4	199	203.2	273	240.7
m_W reconstr.	65	66.98	114	157.5	119	135.4	175	156.5
y_{cut}	55	56.31	89	119.7	106	123.4	157	144.9
cos (vis. p)	44	49.60	77	106.0	91	110.2	137	128.8
hadronic mass	22	20.96	17	19.48	24	24.78	35	28.85
prob of b-jet	1	1.877	1	1.677	3	1.968	3	2.466

Table 7: Number of events with reconstructed top mass as given in the first paragraph of this chapter, remaining after successive application of the selection cuts, for the OPAL data and the background Monte Carlo samples (Bg) for the energy regions 192-196 GeV, 200-202 GeV, 204-206 GeV and 207-208 GeV. The expected number of events, according to PYTHIA, assuming cross-sections as given in table 6, is also shown. The method of recoil of the candidate c-quark is used for the reconstruction of the top mass.

of uncertainties due to modelisation of the signal process. The two Monte Carlo samples give slightly different predictions: with the nominal cuts, the 95% C.L. limits are: 414 fb for PYTHIA and 336 fb for EXOTIC. We take the difference as a systematic uncertainty on the simulation of a signal by Monte Carlo.

- **mass calibration**. Table 7 indicates that, with only the preselection, more data is observed than is expected from backgrounds. Fig. **??**, which shows the reconstructed top mass at this stage of selection, suggests that a mass miscalibration of about 1.5 GeV for low-energy jets (high recoil mass) could explain this disagreement. If an energy shift of 1.5 GeV is imposed on the data, the expected background is comparable or slightly higher than the observed number of events, as cuts are successively applied. With all cuts, there remains still 2 candidate data events for an expected background of 3.0.

- **top mass uncertainty**. The PDG [3] reports a top mass of 173.8 $\pm$ 5.2 GeV. In order to account for this uncertainty, we use the Monte Carlo runs with mass 169 GeV and 179 GeV to estimate a systematic error due to the uncertainty on the top quark mass (see table 9).

Adding the systematic uncertainties in quadrature yields the final result:

	Data	Backgr	PYTHIA	μ	μ	μ	σ_{FCNC}
C.L.				68.3%	90%	95%	95%
$192-196$ GeV	1	1.877	1.708	1.05	2.62	3.39	< 0.71
$200-203$ GeV	1	1.677	1.594	1.19	2.77	3.55	< 1.34
$204-206$ GeV	3	1.968	1.716	3.33	5.45	6.28	< 2.20
$207-209$ GeV	3	2.466	1.614	2.83	4.95	5.78	< 2.15

Table 8: Limit on the FCNC cross section supposing a theoretical cross section of 360 fb for the lowest energy region and 600 fb for the other. The cross section is given in pb.

Cut	Data	Bg	PYTHIA	95% CL μ	95% CL σ_{FCNC}
nominal cuts	3	1.96	1.71	6.28	< 2.20
ℓ isolation $E < 2.5$ GeV	3	1.94	1.70	6.30	< 2.22
ℓ isolation $E < 7.5$ GeV	3	1.99	1.72	6.25	< 2.17
$55 <$W$mass < 105$ GeV	4	2.12	1.81	8.13	< 2.69
$65 <$W$mass < 95$ GeV	1	1.68	1.58	3.54	< 1.34
$y_{12} < 0.4$	3	1.85	1.65	6.39	< 2.32
$y_{12} < 0.35$	2	1.65	1.58	5.07	< 1.92
$y_{12} < 0.5$	4	2.09	1.74	7.66	< 2.64
2 jet mass = 20-60 , 85-95 GeV	5	3.85	2.26	7.40	< 1.97
$m_{top} = 169$ GeV	3	1.96	1.50	6.28	< 2.50
$m_{top} = 179$ GeV	2	2.42	2.37	4.31	< 1.09

Table 9: Number of events with reconstructed top mass for the data region $\sqrt{s} = 204-206$ GeV, remaining after application of all cuts, but with one cut modified as shown. The expected number of events, according to PYTHIA assuming a cross-section of 600 fb is also shown. The 95% C.L. upper bound for the cross-section, in pb (statistical only), based on PYTHIA, is shown in the last column ($\sigma = \mu \times 600\text{fb}/S$ where S is the PYTHIA signal.)

$$\sigma(Z \to t\bar{c} + t\bar{u} + \bar{t}c + \bar{t}u) < 7130\text{fb (95\% C.L.)}$$
$$\text{sensitivity: 591 fb}$$

It must be noted that these quoted limits have assumed a 100% branching ratio $t \to$Wb, which is obviously not the case if there exists a FCNC coupling allowing $t \to Zc$. Indeed, if a cross-section of 0.28 pb for the $Z^* \to tq + h.c.$ channel yields a BR of 33% in the $t \to Zq$ channel [7], we estimate (see appendix) that a cross-section σ corresponds to a BR of $\sigma/(\sigma + 0.56$ pb). The corrected limit, assuming a BR$(t \to Zq) = 33\%$, which is the

CDF limit [6], is then

$$\sigma(Z \to t\bar{c} + t\bar{u} + \bar{t}c + \bar{t}u) < 0.646 \text{ pb (95\% C.L.)} \quad (2)$$

6 Conclusions

A search for single top production in OPAL, based on data at $\sqrt{s} = 192 - 207$ GeV. has yielded an upper limit of 0.433 pb, at 95% C.L., with expected sensitivity 0.591 pb, including systematic errors and assuming $\text{BR}(t \to Zq) = 100\%$. Only the leptonic channel of top decay has been used. This result is competitive, but does not improve on the previous limit on the FCNC coupling, from CDF. It needs to be combined with the limit obtained with the hadronic channel of top decay, and with similar analyses of more data at higher center of mass energy.

References

[1] G. Azuelos and G. Karapetian, *"Search for the FCNC decay $Z \to tq$ in the channel $t \to \ell\nu b$"*, OPAL Technical Note TN655, May 2000

[2] T. Sjöstrand, 1994, Computer Physics Commun. **82**, 74.

[3] Particle Data Group, *Review of Particle Physics* in *Eur. Phys. Journal* **C3** (1998), 1

[4] A. Leins and A. Bellerive, "Investigation of Single Top Quark Production at LEP2", CERN preprint

[5] G. Eilam, J. L. Hewett and A. Soni, Phys. Rev. **D44** (1991) 1473; erratum: Phys. Rev. **D59** (1998) 039901;
G. Couture, C. Hamzaoui and H. Kønig, Phys. Rev. **D52** (1995) 1713

[6] Abe et *al.*, CDF Collaboration, Phys. Rev. Lett. **80** (1998) 2525

[7] V.F. Obraztsov, S.R. Slabospitsky and O.P. Yushchenko, Phys. Atom. Nucl. **62** (1999) 108 (hep-ph/9712394)

[8] T. Han and J. L. Hewett, Phys. Rev. **D60** (1999) 074015

[9] R. Tafirout and G. Azuelos, accepted for publication in Comp. Phys. Comm.

[10] H-U Bengtsson, W-S Hou, A. Soni and D-H Stork, Phys. Rev. Lett. **55** (1985) 2762

[11] S. Yamashita, I. Nakamura, *"LB160: Upgraded B-tagging for LEP2"*, OPAL Technical Note TN578, Nov. 1998

[12] G. F. Feldman and R. D. Cousins, *Phys. Rev.* **D57** (1998) 3873

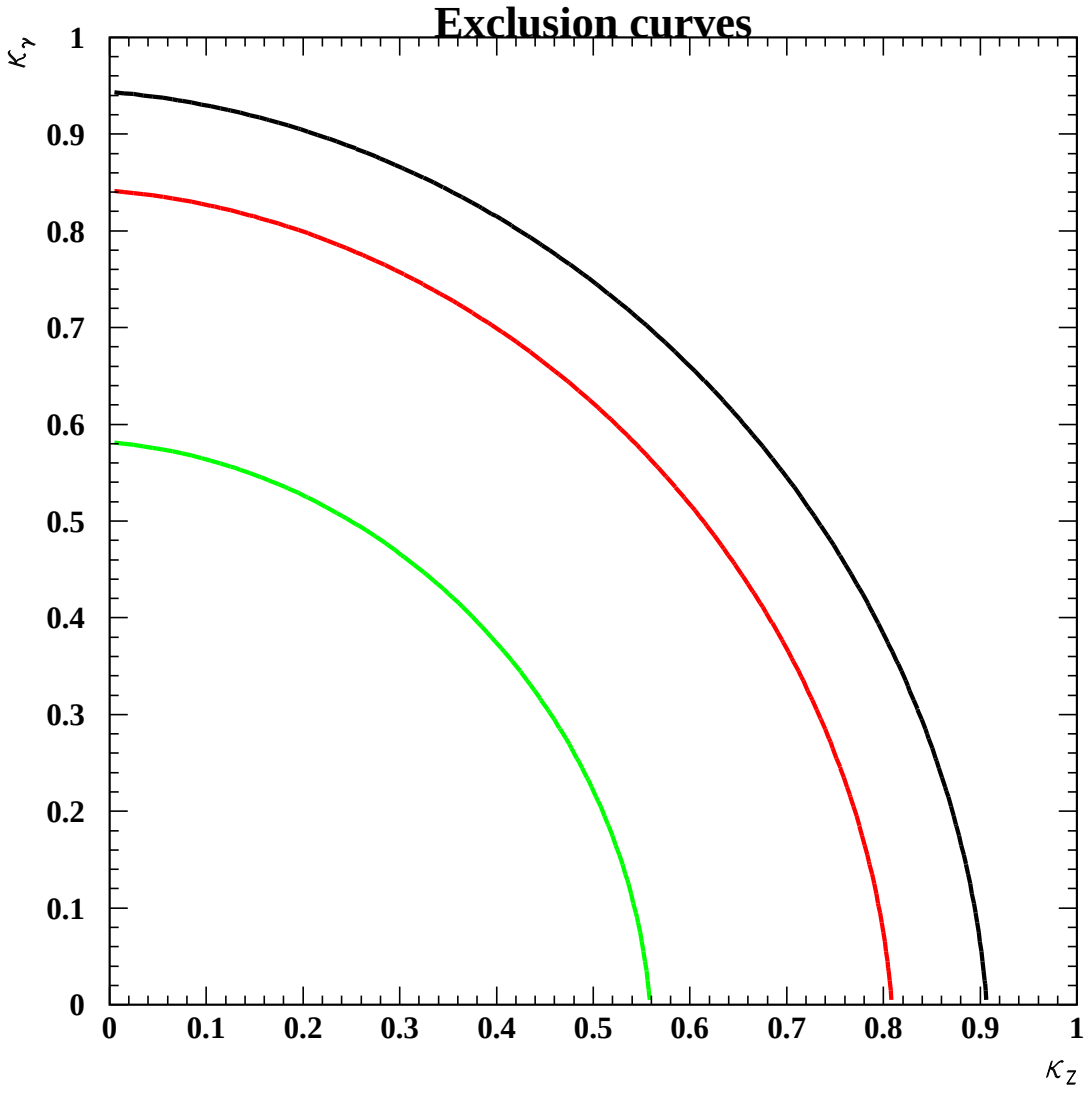

Figure 19: Exclusion curves at 68.3%, 90%, and 95% CL.